International Journal of Advanced Technology and Engineering Exploration, Vol 9(96)
ISSN (Print): 2394-5443 ISSN (Online): 2394-7454
http://dx.doi.org/10.19101/IJATEE.2021.875539

Research Article

FEM based design and performance analysis of 2-poles universal motor

Sudhir Kumar Sharma[1*] and Manpreet Singh Manna[2]
Research Scholar, Department of Electrical and Instrumentation Engineering, Sant Longowal Institute of Engineering and Technology, Sangrur, Punjab, India[1]
Associate Professor, Department of Electrical and Instrumentation Engineering, Sant Longowal Institute of Engineering and Technology, Sangrur, Punjab, India[2]

Received: 23-February-2022; Revised: 12-November-2022; Accepted: 16-November-2022

Abstract
Among various special-purpose motors, the universal motor operates on both supplies, alternating current (AC) and direct current (DC). In this paper, the design of special purpose 2 poles and 100-watt universal motor has been carried out by ANSYS Maxwell software. The focus is on using the rotor pole embrace factor as a design variable; the analysis is done with the help of the parametric approach based on several iterations. The different performance parameters have been taken into account for design analyses like efficiency, torque, speed, and flux density of air gap of the respective motor. Here, the flux pattern and characteristics of the motor with their respective curves was extracted. The electromagnetic analysis of the proposed motor has been analyzed with the help of the finite element method (FEM). Consequently, it is observed that the optimal model offers a significant enhancement in efficiency without bringing additional losses to the motor.

Keywords
Universal motor, ANSYS maxwell, FEM, Parameters, Rotor pole embrace factor.

1.Introduction
In the last few decades, several special purpose electric motors have been designed and explored in a variety of appliances, including mixers, vacuum cleaners, refrigerators, food processors, and hair dryers [1]. Special-purpose motors, such as brushless permanent magnet motors, have recently been a popular research area. Due to their high torque density and efficiency, these are widely employed in industries, particularly in the low to the medium-speed range [2]. However, for high-energy permanent magnets, the significant concerns are price volatility, supply chain difficulties, and environmental repercussions of employing rare earth minerals [3]. Universal motors that do not use permanent magnets are the best alternative to brushless permanent magnet motors and single-phase linear induction motor (LIM). The universal motor is a single-phase motor which is used in small appliances with less power, such as air conditioning blowers and fans, small farming equipment, office machinery, dairy machinery, small power tools, etc. This motor is robust, reliable and capable of operating the tools concerned with power/weight ratio [4−5].

The universal motor is a commutator-type single-phase motor that works on alternating current (AC) and direct current (DC) supplies. The features of this motor are very much like the DC series motor. The main advantage is that it is inexpensive and suitable for a short time with prominent torque characteristics. This motor is beneficial because of its unique characteristics, i.e., high speed and high starting torque. The usual power rating does not exceed 750 W, which is significantly lower than that of other motors. The motor's normal speed rating ranges between 3000 to 20000 revolutions per minute [6−7].

However, the main limitation of the motor is the presence of brushes that lead to hysteresis and eddy current losses. The efficiency of the motor is relatively low compared to other special-purpose motors. The reactance of the field and armature winding is very high, which makes the power factor low, specifically when operating on AC supply [8−9]. So, the main objective of selecting this motor is to

*Author for correspondence

enhance efficiency with the selection of variable parameters in the designing process.

In this paper, a 2-poles universal motor with a 100-watt power rating is designed. While performing the parametric analysis, the embrace factor of rotor pole is considered a design variable to maximize motor efficiency. Finite element-based electromagnetic analysis has been performed using the ANSYS Maxwell to increase the rated torque with the optimum efficiency of the proposed model. The motor designed for optimal value of rotor pole embrace factor, results in fewer losses and highest efficiency compared to other models. The transient analysis along with the electrical analysis was also done with the same tool on the optimal value of the model.

This paper has been divided into several sections. Section 1 illustrates introduction of the motor with various applications. Section 2 focuses on the literature survey of the selected motor. Section 3 emphasis on methods and the mathematical modelling of universal motor. Section 4 deals with the simulated results. Section 5 highlights the discussion of results with the limitations of the present work and Section 6 manifest the conclusions of a proposed model of motor.

2.Literature review

A comprehensive literature review has been conducted to highlight similar applications proposed and implemented during the time frames of ongoing exploration. The researchers demonstrated their interest in the design and mathematical modelling of motors with various computational techniques.

Hsiao et al. [10] designed DC brush motor with an optimized stator structure using finite element method (FEM) based Taguchi algorithm. This technique was beneficial to reduce the magnetic saturation and enhance the output power of the motor for the respective application. However, it remains to be discovered whether the hole's position, shape, and size have a negative effect on the structural safety of the motor body. Kurihara and Koseki [11] designed a new equivalent 4-pole universal motor with finite element analysis (FEA) tool. This design provided better output power and commutation than the existing design based on suitable pole arc coefficient. However, the performance of the motor was analyzed on two parameters, i.e., rated speed and voltage.

Nanhekhan et al. [12] developed the current sensing controller unit for vacuum cleaner application to operate the motor. The advantage of the circuit is its low cost and robust design. Moreover, the same circuit can be operated with AC grid. However, in this study Metal oxide semiconductor field effect transistor (MOSFET) design was used. Further, it can be replaced with insulated gate bipolar transistor (IGBT) device for the energy-efficient circuit. Garg [13] presented a mathematical model of a universal motor based on AC and DC supplies which resulted in better motor performance on DC supply. The study only focused on the electrical characteristics of mathematical modelling and did not opt for other Multiphysics analyses.

Umesh et al. [14] proposed design of universal motor with rotor surface modification (RSM) to reduce acoustic noises and improve the torque parameter with the FEM. The limitation of this work was not employing the finite element adaptivity concept in the design. Sharma and Manna [15] have presented the design of a universal motor for agro applications, resulting in efficiency improvement. The improved design was focused mainly on torque, efficiency, and losses. The authors did not consider parameters like brush angle, number of poles, number of rotor slots etc. Qi et al. [16] proposed a deep slot universal motor for powerful electric tools with an improved commutation spark. However, the speed and efficiency of the motor get reduced with increasing current.

Nayak and Shivarudraswamy [17] presented a model of a brushless direct current (BLDC) motor and universal motor for grinder mixer application. The authors only concentrated on the electrical analysis part of the motors and did not consider the crucial parameter of magnetic analysis. Nayak and Shivarudraswamy [18] compared triode for AC (TRIAC) based universal motor with a voltage source inverter (VSI) to control the speed of the BLDC motor. The design offered better performance and was cost-effective compared to the conventional design. However, the electrical circuitry of the design could not be fitted and compatible with all kinds of motor topologies.

Mercy et al. [19] presented the design of universal motor, which reflected a significant improvement in efficiency and a reduction in heat losses. The thermal analysis was carried out and delivered better results on DC supply than AC supply. Since the authors performed the thermal analysis on the Multiphysics

problem, less emphasis was paid on performance of electrical parameters. Gecer et al. [20] presented the design of switched reluctance motor (SRM), BLDC motor, and induction motor (IM) with ANSYS Maxwell software for electric vehicle applications. The authors demonstrated that the SRM has high torque performance at a high-power value and the BLDC motor has better magnetic field density than other motors. Natarajan et al. [21] proposed a universal motor controller with a pulse width modulation (PWM) chopper for washing machine applications. However, an existing circuit can be employed with a solar photo voltaic system to reduce the power demand.

Benedik et al. [22] developed an approachable method to predict the life and failure reasons of the high-speed bearings used in the universal motor. However, a single platform was used to analyze the issue, which could cause uncertainty in the designed motor. Araga et al. [23] discussed operating characteristics of universal motor with experimental equipment for AC and DC supplies. However, it was observed that the obtained results were inconsistent, which led to overheating during operation and mechanical vibrations. Girovsky and Kanuch [24] presented the effect of AC and DC supplies on universal motor characteristics like speed, efficiency, torque, and electromagnetic radiation. The universal motor offered an increase in efficiency and torque for DC supply, and at AC supply, the universal motor has high electromagnetic field radiation. The authors discussed the generalized modelling of the motor only and did not design the controller and other perspectives.

Li and Zhu [25] proposed a design strategy to elucidate the effect of different design variables on the target using parametric analysis. A generalized system design solution has been discussed, but no in-depth study has been carried out. Liu et al. [26] and Tian et al. [27] presented the parametric analysis technique that examined various issues, including thermodynamics, structural noise and vibration, thermal environment studies in buildings, and others. Electromagnetic field analysis was carried out laterally, which was responsible in determining other stability factors on account of magnetic forces applied on the motor. Sharma and Manna [28] simulated the universal motor with AC and DC supplies to analyze the torque-speed features along with motor proficiency. The authors analyzed the performance of the motor based on torque and speed parameters only but did not consider the variable or external load.

The literature concludes that the universal motor is designed only for small-scale industrial and domestic applications. Out of all the motors, the universal motor, a special-purpose motor, is selected and designed with FEM to enhance the performance for various applications. FEM is an accurate and easy technique for solving Multiphysics problems in large-scale operations. It is observed that the universal motor is less efficient than other motors, and there is a scope for improvement of motor performance.

3.Methods

Initially, the field of electrical machine design used to develop the magnetic circuit model of the machine for the analysis of the different parameters. However, the circuit technique was unable to analyze all the parameters related to the electromagnetic domain of the machine, and it became necessary to use advanced techniques. Designing a motor before building saves the consumption of time and money. The use of computer technology, significantly reduce the designer's workload [29, 30]. Computational electromagnetic is being used more frequently due to the growing use of digital computers to solve electromagnetic difficulties. Therefore, problems can be solved using digitally enabled computers before being carried out in the real world, saving time and money [31, 32]. In the midst of various numerical methods, FEM is best suited for examining rotating electrical machines because of its many advantages. Simultaneously, the FEA tool could help designers and researchers in the realization of electromagnetic calculations and simulating motor performance more precisely [33]. Numerical approaches can be used to solve real world electromagnetic problems. It may take several attempts to incorporate parameter changes into the machine's optimal design before the machine's performance is sufficient [34]. To perform statics-magneto and electrostatic analysis with non-linear materials, such as permanent magnets, steady-state eddy currents, transient eddy currents, motional eddy currents, stress and thermal analysis, FEM-based tools have pre-processing and post-processing components. Analytical equations have been used to suggest numerous analytical models [35]. Researchers report that FEM has been used for various machines; the universal motor can also be employed with this method. There are three main steps to perform FEA.

The first step in FEM is pre-processing where entire geometrical domain and variable-based elucidation

have been completed. The model domain is discretized into several finite elements and nodal equations that correspond to them are developed. Processing is the second stage, during which the actual analysis or solution is completed. The necessary analysis mode is configured based on the dynamic or static loading conditions and the material specifications like linear or non-linear analysis, model analysis, and static analysis. Following the definition of the software type or the solution state, this step concludes with the implementation of the actual solution [36−39]. The final stage is post-processing, wherein software comprises elegant procedures for selecting, printing, charting, and comparing the outcomes acquired at the processing level with analytical data. Following that, a junction error analysis is performed. The outcomes are presented in graphical, visual, or spreadsheet form [33, 39].

The working of the universal motor is similar to a DC series motor, the armature winding (rotor) circuit and the field winding (stator) circuit are connected in series and receive the supply current through brushes, as shown in *Figure 1*. The magnetic fields in the rotor and stator will change directions instantaneously when the supply current direction is reversed. As a result, the torque is not changed, so the universal motor run on AC supply. The motor typically includes a high inertia flywheel coupled to the shaft to smooth rotation against this torque ripple because of the pulsating nature of the torque. Additionally, there are many separate windings on the armature and many segments of the commutator. Because of this, the armature winding inductance is minimized, which helps the motor produce less current and power when it is connected to an AC supply [40, 41].

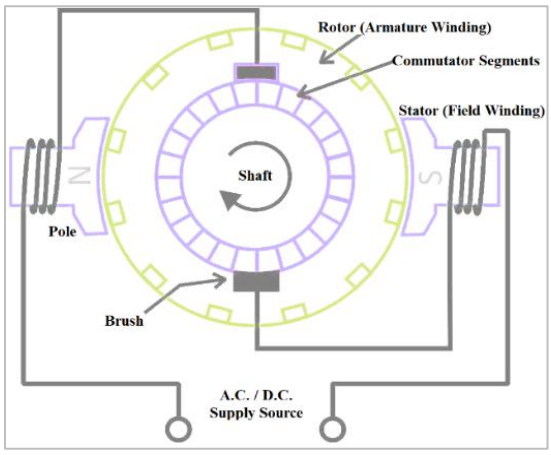

Figure 1 Generalized diagram of universal motor

The equivalent circuit diagram of the universal motor is shown in *Figure 2*. The operating conditions, i.e., voltage and current equations of universal motor, are similar to DC series motor. The generalized mathematical equations related to the universal motor have been discussed in this section. The field current, and armature current are equal to supply current as mentioned in Equation 1.

$$I = I_f = I_a \quad (1)$$

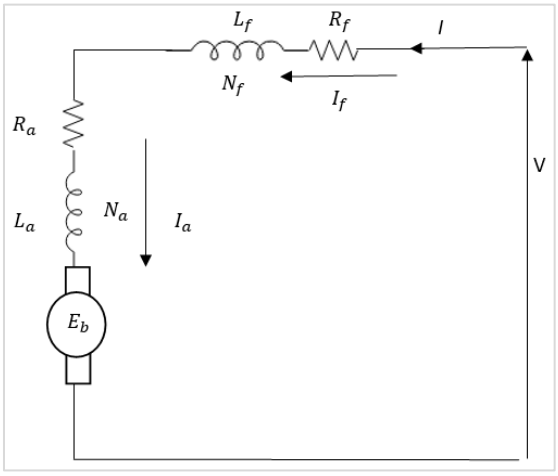

Figure 2 Universal motor equivalent circuit

The equation related to armature winding voltage drop, back emf across armature, voltage drop due to mutual inductance, field winding voltage drop, and voltage drop due to brushes are mentioned in the Equation 2, Equation 3, Equation 4, Equation 5, and Equation 6 respectively.

$$V_a = R_a I_a + L_a (dI_a/dt) \quad (2)$$
$$E_b = \Phi ZNP/60A \quad (3)$$
$$E_m = L_{af} (dI/dt) \quad (4)$$
$$V_f = R_f I_f + L_f (dI_f/dt) \quad (5)$$
$$V = V_a + V_f + E_m + E_b + V_{bd} \quad (6)$$

In above mentioned equations, I = load current, I_f = current of field winding, I_a = armature winding current, V_a = armature's voltage drops, R_a = armature winding's resistance, L_a = armature winding's inductance, E_b = back emf, Φ = flux produced per pole, Z = total number of armature conductors, N = rotational speed of armature in revolutions per minute, P = number of poles, A = number of parallel paths in armature, E_m = voltage drop due to mutual inductance, L_{af} = mutual inductance between armature and field windings, V_f = field's voltage drops, R_f = field winding's resistance, L_f = field winding's inductance, V = supply voltage, V_a = armature's voltage drops, and V_{bd} = voltage drop due to brushes.

3.1Power loss

Efficiency is the ratio of output to input powers, it is depend on different types of losses, such as copper loss, iron loss, mechanical loss, and brush loss. The mechanical loss and brush loss are depended on speed of the motor.

3.1.1Copper loss

The copper loss occurred when current passes through copper conductors. The armature and field winding losses are two types of copper losses. Copper loss of armature and field winding can be determined in Equation 7 and Equation 8 respectively.

$$P_{arm.\_cu} = I_a^2 R_a \quad (7)$$

$$P_{field\_Cu} = I_f^2 R_f \quad (8)$$

3.1.2Iron loss

The alternating magnetization of the magnet core causes iron losses, which is the summation of hysteresis and eddy current loss. The eddy current loss (P_e) and hysteresis loss (P_h) can be calculated by using Equation 9 and Equation 10 respectively.

$$P_e = k_e B^2 f^2 v \quad (9)$$

$$P_h = k_h B^n f v \quad (10)$$

k_h = material-dependent coefficient of hysteresis, B = flux density maximum, n = Steinmetz exponent of material-dependent, f = frequency, v = magnetic material volume, and k_e = material-dependent coefficient of eddy current

The design of the universal motor has done with the ANSYS Maxwell software. The flow chart of design procedure of the universal motor model is shown in *Figure 3*.

The first step is to design the geometry of the motor with the pre-requisite values of the parameters. The parametric analysis was performed on the design variable of the rotor pole embrace factor. The iterations on the variable impact the output performance of the motor. If the performance does not match, then the variable function needs to be updated.

4.Results

4.1Design specifications of motor

The general pre-requisite parameters for the design of a universal motor in RMxprt are mentioned in T*able 1*, these parameters are used as the input to the software to design the motor, and the basic structure model of the universal model is shown in *Figure 4.* The number of poles is 2, type of steel used is steel_1010, which has good thermal stability.

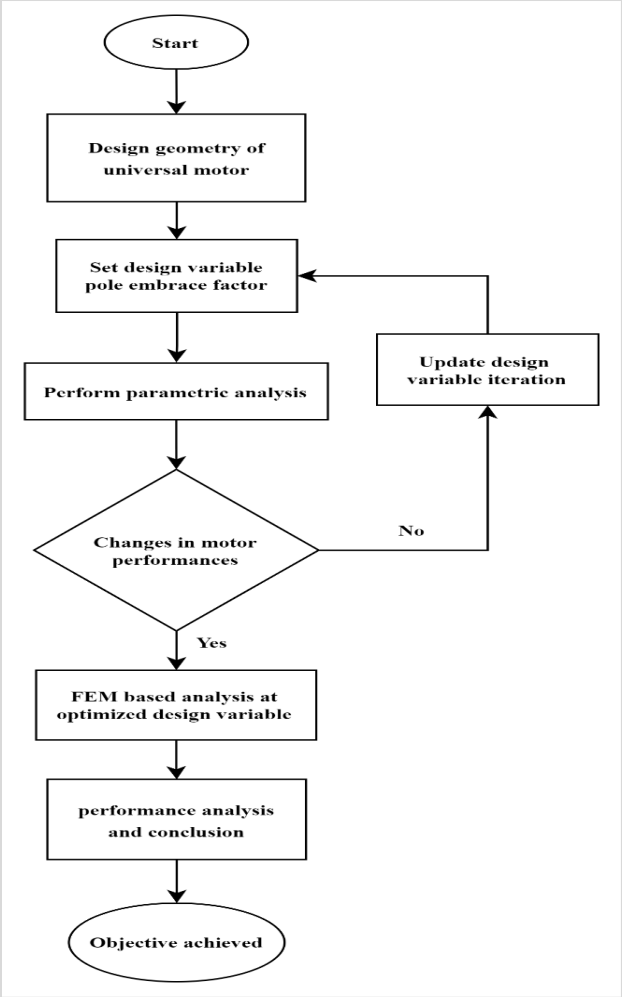

Figure 3 Flow chart of the design procedure

Table 1 Prerequisite parameters of universal motor

S. No.	Parameter	Value
1	Pole number	2
2	Stator outer diameter (mm)	61.5
3	Stator inner diameter (mm)	38.5
4	Stator stack length (mm)	33.35
5	Rotor outer diameter (mm)	35.5
6	Rotor inner diameter (mm)	12.1
7	Rotor stack length (mm)	33.5
8	Type of material	Steel_1010

The technical specifications required for the motor are mentioned in *Table 2*.

Table 2 Technical requirements of universal motor

S. No.	Parameter	Value
1	Rated voltage	120 volts
2	Rated speed	12400 rpm
3	Rated power	100 watt
4	Frequency	60 Hz

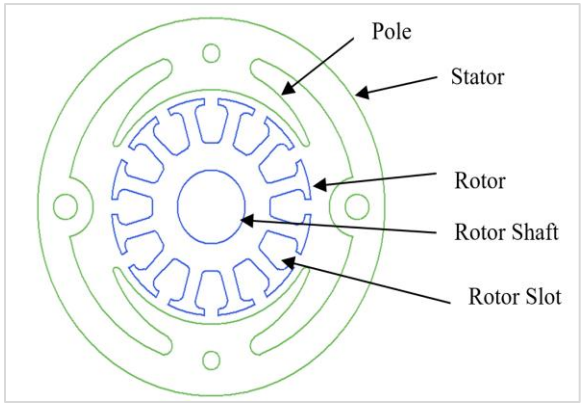

Figure 4 Basic structure of 2-poles universal motor

4.2Results of the motor

The variable design factor chosen for this model is a factor of the pole embrace of the rotor, defined as the fractional ratio of the pole pitch to the pole arc coefficient. The value of the pole embrace factor must be less than unity [42−45], and for this particular design, the initial value taken for the model is 0.5. The representation of this is shown in *Figure 5*.

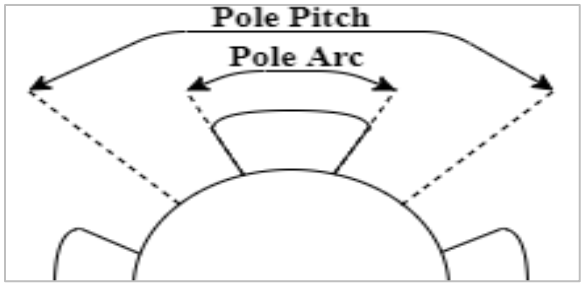

Figure 5 Diagram of pole embrace factor

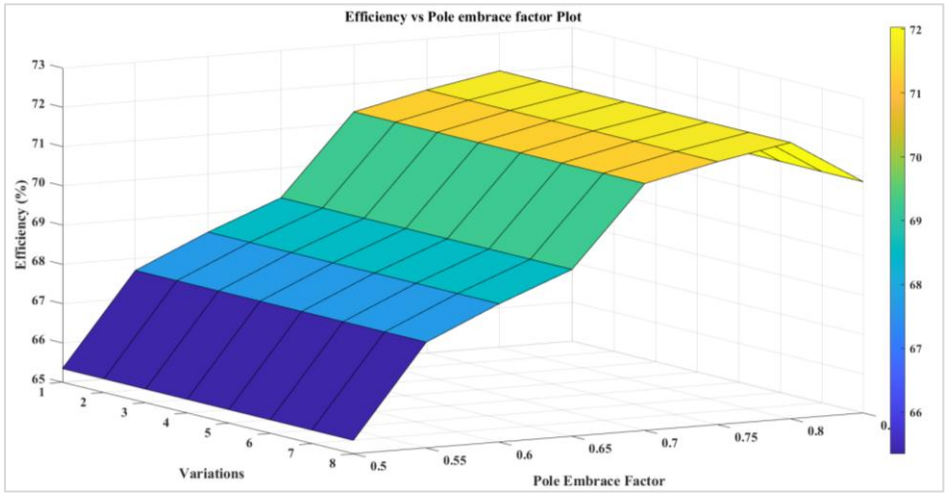

Figure 6 Efficiency vs. rotor pole embrace factor plot

The motor performance is analyzed with variation of the pole embrace factor of rotor represented. The initial value of variable is selected as 0.5. Through the aid of the parametric analysis, step iteration of value 0.05 taken, and the value is varied from 0.5 to 0.85. The sensitivity analysis of the parameter varies from 0.5 to 0.85 as the particular model has less sensitive at other values. Based upon this variation, the performance parameters like efficiency, total losses, rated torque, rated speed, and air gap flux density are analyzed. Thus, the pole embrace factor values meeting the minimum total losses and maximum efficiency have been found for each discrete solution method. The plots of these performance parameters are shown in *Figure 6* to *Figure 10* with respect to the pole embrace factor.

The region where the efficiency is maximum should be addressed during the parametric approach-based process of optimizing the embrace values. However, finding the value that offers maximum efficiency while minimizing losses is not always simple. In such instances, one should decide based on the design priorities. If the reduced losses value results in reduced efficiency, new values should be defined that do not cause the efficiency to decline and preserve the value of rated torque within the pre-determined range. From *Figure 6* and *Figure 7*, it is observed that at the pole embrace factor value 0.8 the motor has the highest efficiency and lowest losses, in comparison to the initial value 0.5. The rated torque is maximum 0.85 and minimum at 0.5 as shown in *Figure 8*.

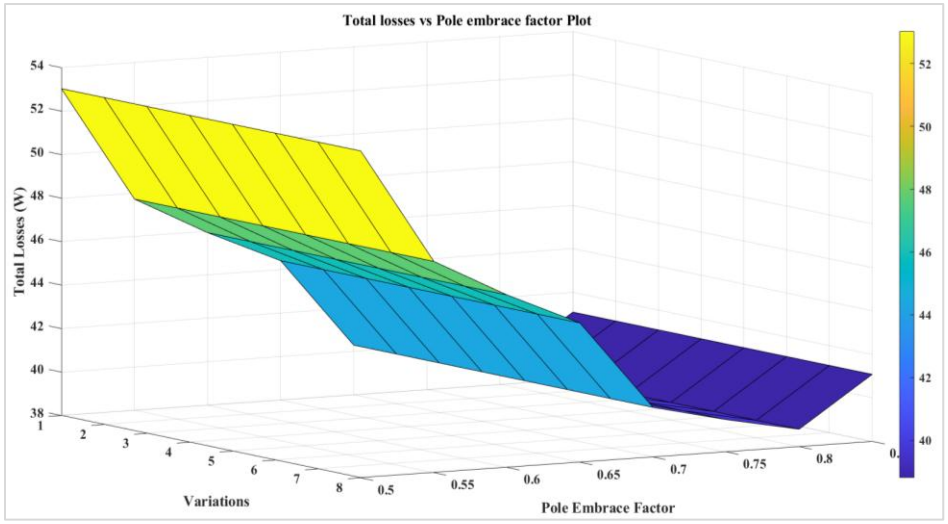

Figure 7 Total losses vs. rotor pole embrace factor plot

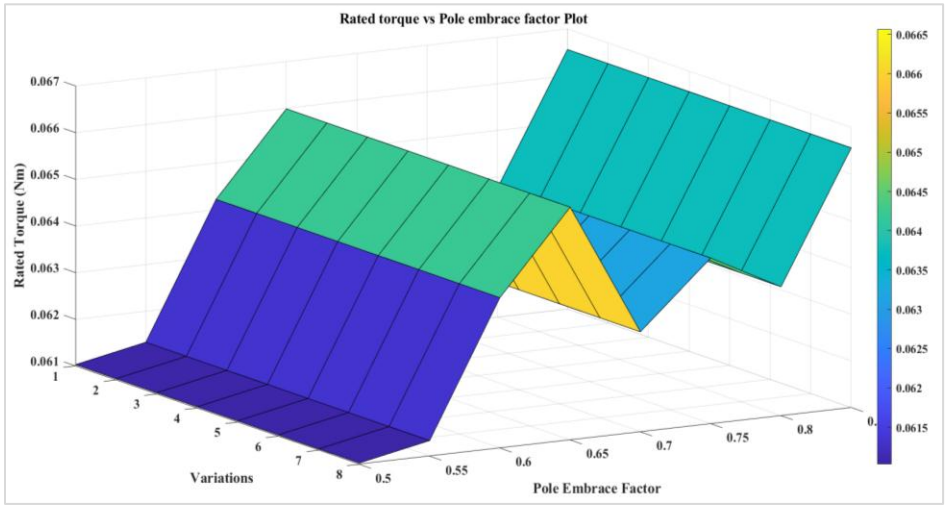

Figure 8 Rated torque vs. rotor pole embrace factor plot

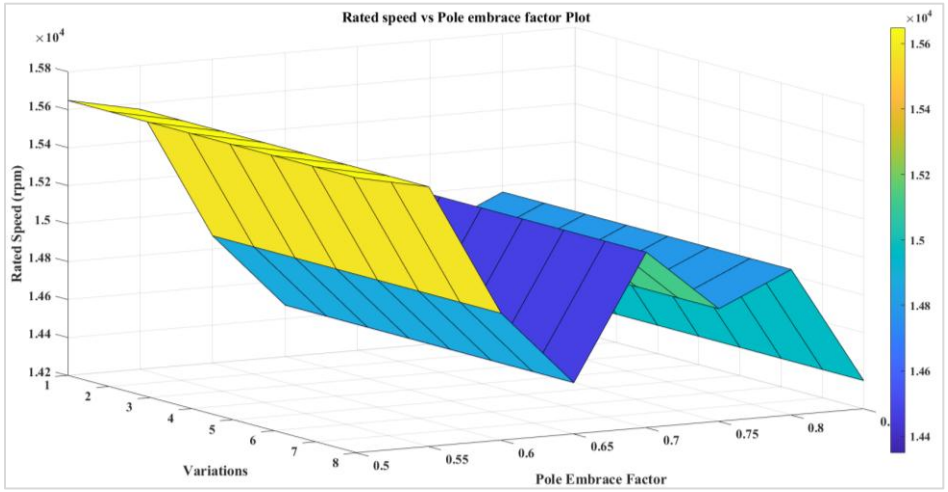

Figure 9 Rated speed vs. rotor pole embrace factor plot

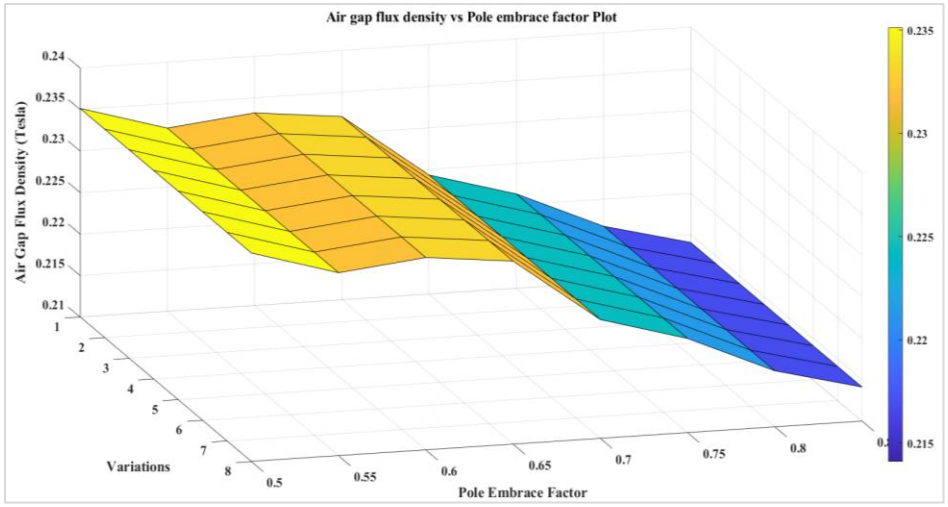

Figure 10 Air gap flux density vs. rotor pole embrace factor plot

Figure 9 shows that the rated speed is maximum at 0.5 and minimum at 0.85. The air gap flux density is minimum at value 0.85 and maximum at 0.5 as shown in *Figure 10*. It should be noted that the designer carefully needs to decide the limits of the solution range since the motor efficiency will fall below 70% for value 0.5 to 0.65.

5.Discussion

The comparative analysis of the results in tabular form is shown in *Table 3*. It shows that the efficiency has improved from 65.3% to 72.03%, with minimum losses in value 0.8. The rated speed at this point is 1434.7 rpm with rated torque of 0.063 Nm and air gap density of 0.21675 T. As pole arc increases, the surface area of pole increases, this implies increment in pole embrace value, which affects the air gap flux density in decreasing manner. The decrement of air gap flux density requires low current. This low current is responsible for less losses, affecting efficiency in an increasing manner. The rated speed varies inversely proportional to rated torque to maintain constant power output. But after because model achieves a saturation point, so the efficiency of the model 8 starts decreasing.

Some important graphs are discussed below when the model simulation was executed in the RMxprt. Critical performance data such as efficiency versus speed, output torque versus speed, and output power versus speed, can be quickly calculated at the optimal point 0.8 of the model. These various graphs of the model's performance are shown in the *Figure 11*, *Figure 12* and *Figure 13*, respectively.

The variation of the performance data is seen with the variation of the speed. *Figure 11* shows the efficiency of the motor decreases after rated speed and increases before rated speed. *Figure 12* shows that output torque is inversely proportional to varying with respect to speed. *Figure 13* shows output power with respect to speed graph.

Table 3 Comparative analysis of results

S. No.	Variations	Variable (R_pem)	Efficiency (%)	Total losses (W)	Rated torque (Nm)	Rated speed (rpm)	Air gap flux density (Tesla)
1	Model 1	0.5	65.3462	53.0344	0.06103	15648.6	0.23513
2	Model 2	0.55	67.6959	47.7164	0.06133	15568.5	0.23206
3	Model 3	0.6	68.5238	45.9347	0.06422	14868.9	0.23319
4	Model 4	0.65	69.2489	44.4055	0.06599	14470.6	0.23206
5	Model 5	0.7	71.2873	40.2817	0.06314	15124.7	0.22432
6	Model 6	0.75	71.6946	39.4815	0.06455	14793.5	0.22134
7	Model 7	0.8	72.0334	38.8007	0.06376	14967.4	0.21675
8	Model 8	0.85	70.8844	41.0832	0.06657	14348.7	0.2141

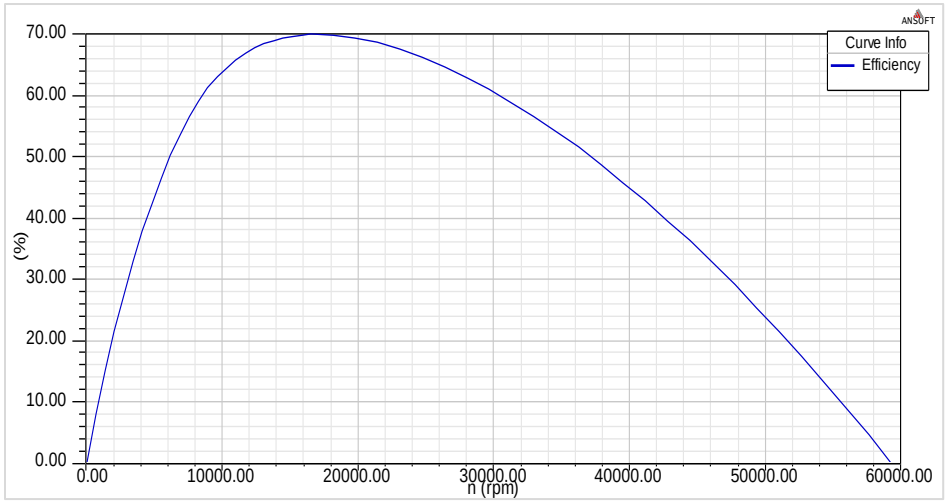

Figure 11 Efficiency versus speed curve

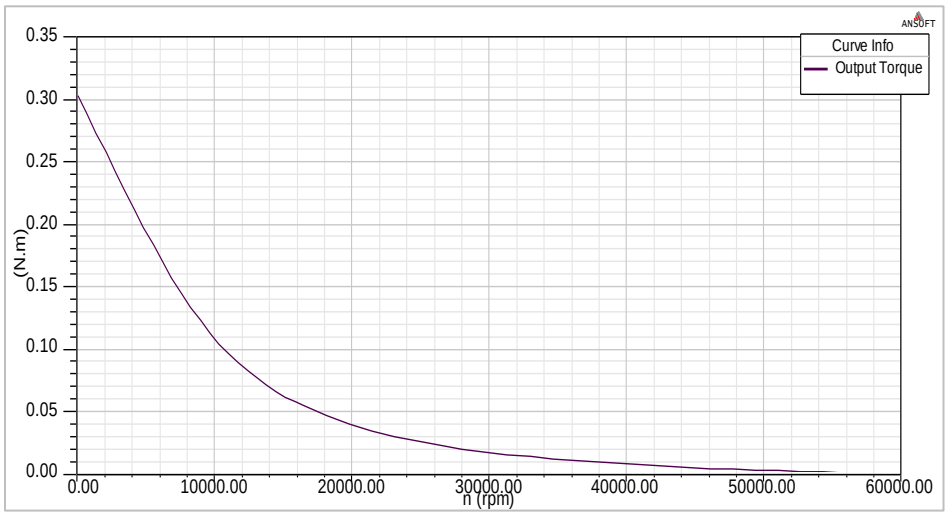

Figure 12 Output torque versus speed curve

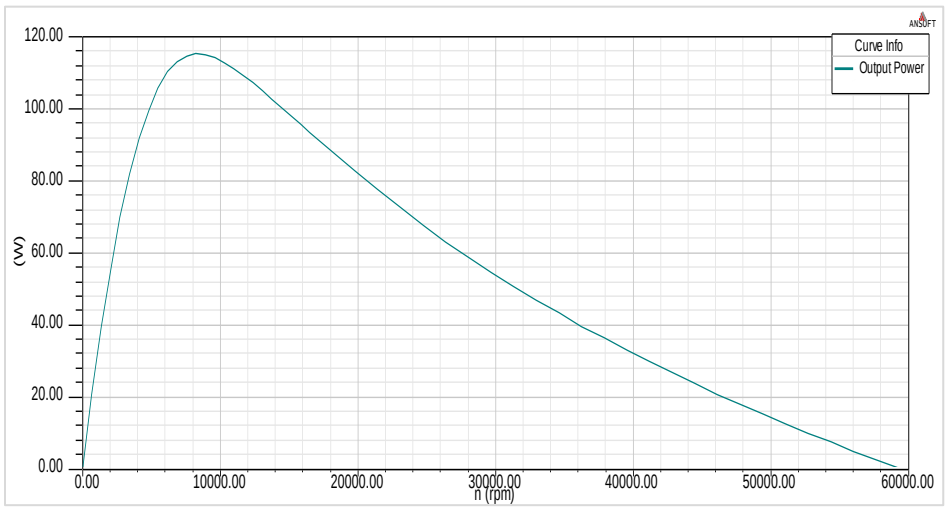

Figure 13 Output power versus speed curve

The motor design created on RMxprt is transformed into Maxwell two dimensional (2D). At output power and rated speed, the optimal model design generated for the optimal embrace factor value derived from the optimization is subjected to 2D transient FEM evaluations. The electromagnetic analysis is done with the help of Maxwell 2D. The magnetic flux density distribution at a specific time of rotor position is shown in *Figure 14.* The magnetic field density of the motor is approximately achieved and it can be interpreted that the distribution is varied at various positions of the motor. The magnetic field lines are shown in *Figure 15* at specific boundaries of rotor and stator of the motor at specific time of rotor position. The magnetic field vector potential of the 2-poles universal motor is shown in *Figure 16.* The flux density lines start from the north pole moving towards the south pole of the motor having high density in the boundary at the motor pole. As a result, the motor size is limited, and it is also ensured that the motor does not function at a flux density close to saturation. These criteria are necessary for thoroughly examining ideal motor design characteristics. *Figure 17* shows the variation of induced rms current in a winding of motor with respect to time. A complete list of abbreviations is shown in *Appendix I.*

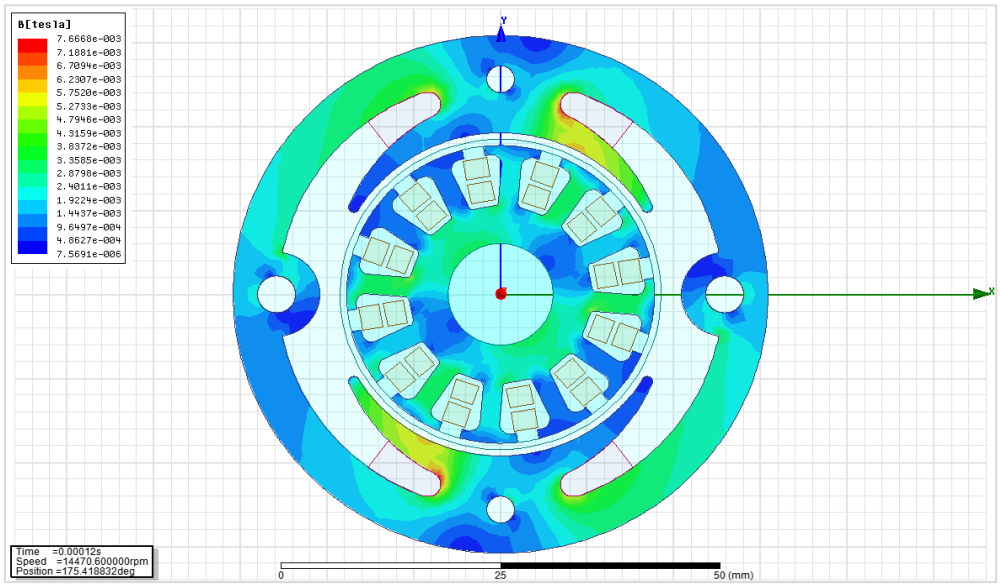

Figure 14 Magnetic flux density at specific time of rotor position

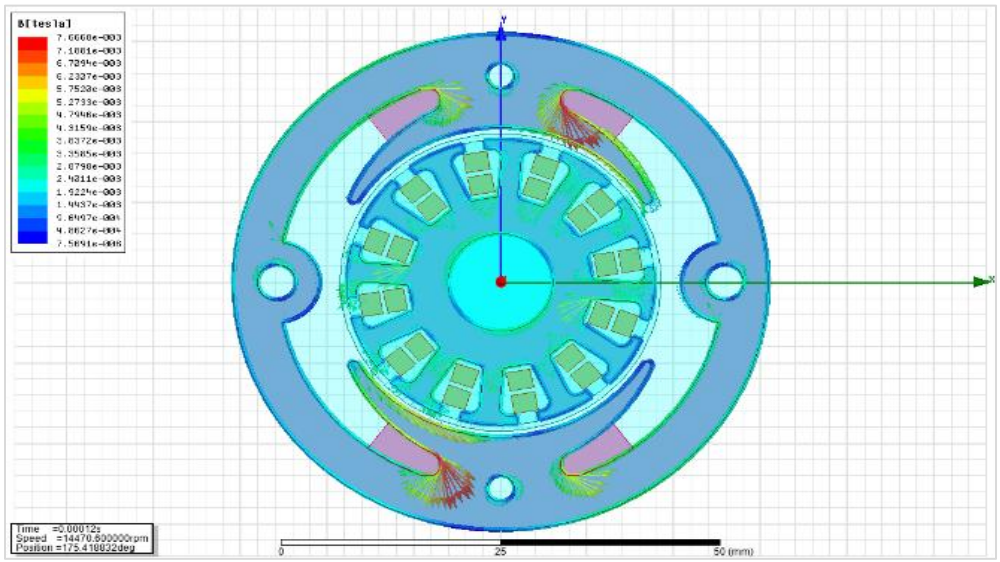

Figure 15 Magnetic field lines at specific time of rotor position

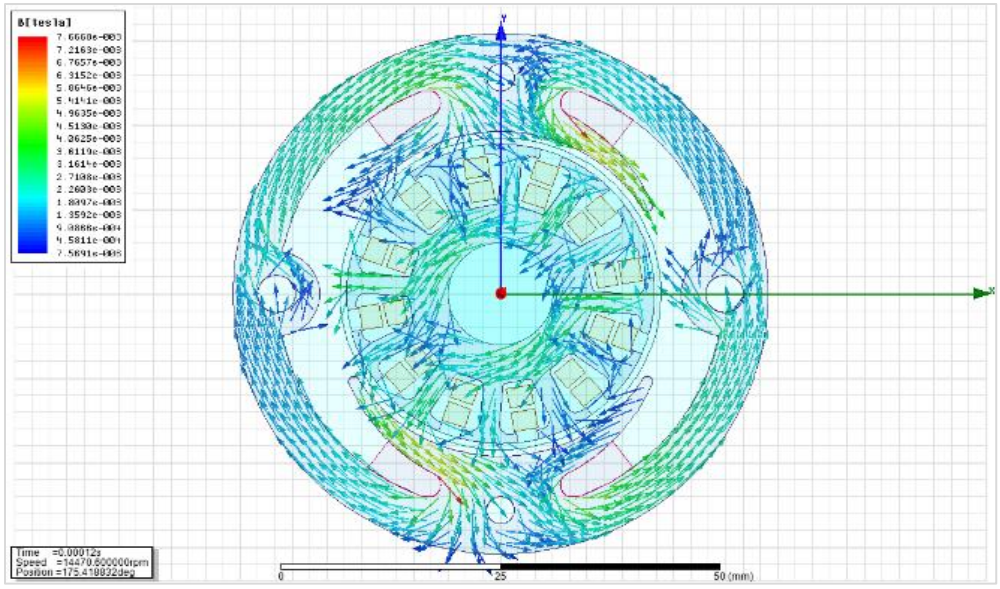

Figure 16 Magnetic field vector potential at specific time of rotor position

The main drawback is that the design rating of universal motor cannot go beyond 1kW with 2 or 4 pole only. Its size is compact and used for small operations. The motor cannot run without load, and the starting speed is very high. This motor has high losses when the operating supply is AC as it has high reactance losses. As compared to other special purpose motors, this particular motor has low efficiency.

Figure 17 Induced current versus time curve

6.Conclusion and future work

The performance analysis of the 100-watt universal motor running at 12400 rpm speed is analyzed with the help of FEM tool. The parametric analysis is applied to the motor and performance of parameters achieved with data curves based on changing patterns. In the comparative analysis, it is realized that the motor has the highest efficiency of 72.0334% and minimum losses of approximately 38 watts at 0.8 compared to the other values. So, this value is selected as the optimal value upon which the FEM model of the motor is designed. The flux density of

the motor is also realized with their directions and patterns. Further, we can select more than one variable to enhance the motor's performance and minimize the losses created at high speed. With current proposed work to improvise the design these may opt for many applications in industry as well as agriculture solutions to give economical and reliable operational results of motor.

Acknowledgment
Sant Longowal Institute of Engineering and Technology, Punjab and All India Council for Technical Education (AICTE), India, are acknowledged for supporting this work.

Conflicts of interest
The authors have no conflicts of interest to declare.

Author's contribution statement
Sudhir Kumar Sharma: Conceptualization, investigation on challenges, data analysis, data acquisition and writing the original draft. **Manpreet Singh Manna:** Interpretation of results, review, supervision, reading proof and the revision of the whole article.

References
[1] Hussain A. Electrical machines. Dhanpat Rai and Co., Educational and Technical Publishers; 2005.
[2] Bilgin B, Emadi A. Electric motors in electrified transportation: a step toward achieving a sustainable and highly efficient transportation system. IEEE Power Electronics Magazine. 2014; 1(2):10-7.
[3] Liu C. Emerging electric machines and drives-an overview. IEEE Transactions on Energy Conversion. 2018; 33(4):2270-80.
[4] Orisaleye JI, Jekayinfa SO, Ogundare AA, Adefuye OA, Bamido E. Effect of screen size on particle size distribution and performance of a small-scale design for a combined chopping and milling machine. Cleaner Engineering and Technology. 2022; 7:1-10.
[5] Ryff PF, Platnick D, Karnas JA. Electrical machines and transformers: principles and applications. Prentice-Hall; 1987.
[6] Grop H. Modelling of a universal motor with speed control. Master, Department of Electrical Engineering Electrical Machines and Power Electronics, Royal Institute of Technology, Stockholm. 2006.
[7] Sen PC. Principles of electric machines and power electronics. John Wiley & Sons; 2007.
[8] Lin D, Zhou P, Stanton S. An analytical model and parameter computation for universal motors. In international electric machines & drives conference 2011 (pp. 119-24). IEEE.
[9] Di GA, Perini R. The universal motor: a classic machine with evergreen challenges in design and modeling. In workshop on electrical machines design, control and diagnosis 2013 (pp. 85-94). IEEE.
[10] Hsiao HC, Hsiao CY, Chen GR. Finite element analysis and optimal design of DC brush motor for automotive engine start applications. In student conference on electric machines and systems 2019 (pp. 1-5). IEEE.
[11] Kurihara K, Koseki S. New design of high output equivalent 4-pole universal motor. In international conference on electrical machines 2018 (pp. 291-6). IEEE.
[12] Nanhekhan B, Woudstra J, Van DP. Brushed universal motor controller for DC-grids. In 19th international conference on research and education in mechatronics 2018 (pp. 153-8). IEEE.
[13] Garg R. Behavioral analysis of a universal motor when operated on DC and AC supply. In international conference on intelligent computing and control systems 2019 (pp. 705-10). IEEE.
[14] Umesh V, Mishra S, Simon S, Singh AK, Moses P. Universal electrical motor acoustic noise reduction based on rotor surface modification. In international conference on data science and communication 2019 (pp. 1-5). IEEE.
[15] Sharma SK, Manna MS. Finite element electromagnetic based design of universal motor for agro application. International Journal of Electrical and Electronics Research. 2022; 10(3):590-6.
[16] Qi H, Ling L, Jichao C, Wei X. Design and research of deep slot universal motor for electric power tools. Journal of Power Electronics. 2020; 20(6):1604-15.
[17] Nayak DS, Shivarudraswamy R. Loss and efficiency analysis of BLDC motor and universal motor by mathematical modelling in the mixer grinder. Journal of the Institution of Engineers (India): Series B. 2022; 103(2):517-23.
[18] Nayak DS, Shivarudraswamy R. Efficiency and loss analysis of proposed BLDC motor drive and existing universal motor drive used in a mixer grinder. International Journal of Mechanical Engineering and Robotics Research. 2020; 9(6):808-12.
[19] Mercy A, Umamaheswari B, Latha K. Reduced-order thermal behavior of universal motor-driven domestic food mixers/grinders using AC and DC supplies. Journal of Power Electronics. 2021; 21(9):1322-32.
[20] Gecer B, Tosun O, Apaydin H, Serteller NF. Comparative analysis of SRM, BLDC and induction motor using ANSYS/maxwell. In international conference on electrical, computer, communications and mechatronics engineering 2021 (pp. 1-6). IEEE.
[21] Natarajan S, Balasubramanian K, Satpathy PR, Babu TS. Universal motor with on-off controller for washing machine application. In international conference in advances in power, signal, and information technology 2021 (pp. 1-6). IEEE.
[22] Benedik B, Rihtaršič J, Povh J, Tavčar J. Failure modes and life prediction model for high-speed bearings in a through-flow universal motor. Engineering Failure Analysis. 2021; 128:1-17.
[23] Araga IA, Airoboman AE, Inalegwu AP, Afolayan IA, Adunola FO. A comparative analysis on the performance of universal motor when driven by alternating current/direct current. Australian Journal of Science and Technology. 2020; 4(4):348-52.

[24] Girovský P, Kaňuch J. Analysis of the power supply influence on the universal motor. Power Electronics and Drives. 2022; 7(42):103-11.
[25] Li E, Zhu J. Parametric analysis of the mechanism of creating indoor thermal environment in traditional houses in Lhasa. Building and Environment. 2022.
[26] Liu X, Zhang N, Sun Q, Wang K, Wu Z. Parametric analysis of structural noise of steel-concrete composite slab beams. Shock and Vibration. 2022.
[27] Tian L, Wu L, Huang X, Fang Y. Driving range parametric analysis of electric vehicles driven by interior permanent magnet motors considering driving cycles. CES Transactions on Electrical Machines and Systems. 2019; 3(4):377-81.
[28] Sharma SK, Manna MS. Performance analysis of universal motor based on MATLAB simulation. In international conference for advancement in technology 2022 (pp. 1-4). IEEE.
[29] Cros J, Viarouge P, Chalifour Y, Figueroa J. A new structure of universal motor using soft magnetic composites. IEEE Transactions on Industry Applications. 2004; 40(2):550-7.
[30] Chan CC, Chau KT. Design of electrical machines by the finite element method using distributed computing. Computers in Industry. 1991; 17(4):367-74.
[31] Madenci E, Guven I. The finite element method and applications in engineering using ANSYS®. Springer; 2015.
[32] Sadiku MN. Numerical techniques in electromagnetics. CRC Press; 2000.
[33] Zienkiewicz OC, Taylor RL, Zhu JZ. The finite element method: its basis and fundamentals. Elsevier; 2005.
[34] Tezcan MM, Çanakoğlu AI, Yetgin AG, Gün A, Cevher B, Turan M. Analysis of one phase special electrical machines using finite element method. In international conference on electromechanical and power systems 2017 (pp. 113-8). IEEE.
[35] Knight AM, Salmon JC, Ewanchuk J. Integration of a first order eddy current approximation with 2D FEA for prediction of PWM harmonic losses in electrical machines. IEEE Transactions on Magnetics. 2013; 49(5):1957-60.
[36] Morin P, Nochetto RH, Siebert KG. Convergence of adaptive finite element methods. SIAM Review. 2002; 44(4):631-58.
[37] Sykulski J. Computational electromagnetics for design optimisation: the state of the art and conjectures for the future. Bulletin of the Polish Academy of Sciences: Technical Sciences. 2009; 57(2).
[38] Raja CV, Sudha KR. Design, analysis of linear induction motor based on harmony search algorithm and finite element method. Journal of Engineering Science and Technology Review. 2016; 9(6):189-95.
[39] Kumar A, Marwaha S, Marwaha A. Finite element 2D steady-state time harmonic field analysis of induction motor. In proceedings of the IEEE INDICON, 2004 (pp. 570-4). IEEE.
[40] Sawhney AK, Chakrabarti A. Course in electrical machine design. Dhanpat Rai; 2010.
[41] Abdeljawed HB, El Amraoui L. Simulation and rapid control prototyping of DC powered universal motors speed control: towards an efficient operation in future DC homes. Engineering Science and Technology, an International Journal. 2022.
[42] Marwaha S. Mitigation of cogging torque for the optimal design of BLDC motor. In IEEE 2nd international conference on electrical power and energy systems 2021 (pp. 1-5). IEEE.
[43] Zhang Y, Ruan J, Huang T, Yang X, Zhu H, Yang G. Calculation of temperature rise in air-cooled induction motors through 3-D coupled electromagnetic fluid-dynamical and thermal finite-element analysis. IEEE Transactions on Magnetics. 2012; 48(2):1047-50.
[44] Sadrossadat SA, Rahmani O. A framework for statistical design of a brushless DC motor considering efficiency maximisation. IET Electric Power Applications. 2022; 16(3):407-20.
[45] Yildirim M, Kurum H. Influence of poles embrace on in-wheel switched reluctance motor design. In 18th international power electronics and motion control conference 2018 (pp. 562-7). IEEE.

Sudhir Kumar Sharma received the B. Tech degree in Electrical Engineering in 2015 from Rajasthan Technical University, Kota, India and M. Tech degree in Electrical Engineering in 2019 from Punjab Engineering College, Chandigarh, India. Currently, he is pursuing a Ph.D. degree with the Electrical and Instrumentation Engineering Department, SLIET, Longowal, Punjab, India. His area of interest is Machine Design, Electric Vehicle Application, Power System, and Renewable Sources**.**
Email: sudhirs390@gmail.com

Dr. Manpreet Singh Manna received the B.E. degree in Electrical & Electronics Engineering from P.E.S. College of Engineering, Mandya, Karnataka, India, in 1993, M.E. degree in Power & Machines from Thapar Institute of Engineering & Technology, Patiala, India in 2000 and a Ph.D. degree in Electrical & Instrumentation Engineering from SLIET Longowal, Punjab, India. He was the former Director at AICTE, New Delhi, India. Currently, he is an Associate Professor in the Electrical and Instrumentation Engineering Department at SLIET Longowal, Punjab, India. His area of interest is Power System, Machine Design, and Renewable Sources.
Email: mannasliet@gmail.com

Appendix I

S. No.	Abbreviation	Description
1	AC	Alternating Current
2	BLDC	Brushless Direct Current
3	DC	Direct Current
4	FEA	Finite Element Analysis
5	FEM	Finite Element Method
6	IGBT	Insulated Gate Bipolar Transistor
7	IM	Induction Motor
8	LIM	Linear Induction Motor
9	MOSFET	Metal Oxide Semiconductor Field Effect Transistor
10	PWM	Pulse Width Modulation
11	RSM	Rotor Surface Modification
12	SRM	Switched Reluctance Motor
13	TRIAC	Triode For Alternating Current
14	VSI	Voltage Source Inverter
15	2D	Two Dimensional